

Article

Spatio-Temporal Patterns of the 2010–2015 Extreme Hydrological Drought across the Central Andes, Argentina

Juan Antonio Rivera ^{1,2,*}, Olga C. Penalba ^{3,4}, Ricardo Villalba ¹ and Diego C. Araneo ¹

¹ Instituto Argentino de Nivología, Glaciología y Ciencias Ambientales (IANIGLA), CCT-Mendoza/Consejo Nacional de Investigaciones Científicas y Técnicas (CONICET), Av. Ruiz Leal s/n, 5500 Mendoza, Argentina; ricardo@mendoza-conicet.gob.ar (R.V.); daraneo@mendoza-conicet.gob.ar (D.C.A.)

² Facultad de Ciencias Veterinarias y Ambientales, Universidad Juan Agustín Maza, Av. Acceso Este, Lateral Sur 2245, 5521 Mendoza, Argentina

³ Departamento de Ciencias de la Atmósfera y los Océanos, Facultad de Ciencias Exactas y Naturales, Universidad de Buenos Aires, Intendente Güiraldes 2160, C1428EGA Buenos Aires, Argentina; penalba@at.fcen.uba.ar

⁴ Consejo Nacional de Investigaciones Científicas y Técnicas (CONICET), Godoy Cruz 2290, C1425FQB Buenos Aires, Argentina

* Correspondence: jrivera@mendoza-conicet.gob.ar; Tel.: +54-261-428-6010

Academic Editors: Paulo Barbosa and Jürgen Vogt

Received: 1 June 2017; Accepted: 23 August 2017; Published: 30 August 2017

Abstract: During the period 2010–2015, the semi-arid Central Andes in Argentina (CAA) experienced one of the most severe and long-lasting hydrological droughts on record. Since the snowmelt is the most important source of water, the reduced snowfall over the mountains propagated the drought signal through the streamflows in the adjacent foothills east of the Andes ranges. Motivated by the widespread impacts on the socio-economic activities in the region, this study aims to characterize the recent hydrological drought in terms of streamflow deficits. Based on streamflow data from 20 basins, we used the standardized streamflow index (SSI) to characterize hydrological droughts during the period 1971–2016. We found that the regional extent of the 2010–2015 hydrological drought was limited to the basins located north of 38° S, with mean duration of 67 months and maximum drought severity exhibiting a heterogeneous pattern in terms of spatial distribution and time of occurrence. The drought event reached extreme conditions in 14 of the 15 basins in the CAA, being record-breaking drought in six of the basins. This condition was likely driven by a cooling in the tropical Pacific Ocean resembling La Niña conditions, which generated a decrease in snowfall over the Andes due to suppressed frontal activity.

Keywords: hydrological drought; semi-arid region; streamflow; Central Andes; drought; hydroclimatic variability; water resources; standardized streamflow index; Argentina; snowmelt

1. Introduction

Given the recent changes in the frequency, duration and intensity of droughts, a comprehensive understanding of water scarcity is needed at different temporal and spatial scales. This requirement is pressing given the marked increase in demand of water for agriculture, energy production, industry and human consumption. Droughts occur in virtually all climates, but have larger impacts in arid and semi-arid regions of the world where droughts are characterized by long duration (up to several years) and high intensity [1]. The scarcity of precipitation over an extended period define the meteorological drought, whereas its consequences on the hydrological cycle, such as abnormally

low streamflows, low levels in lakes and reservoirs, and deeper groundwaters, is known as hydrological drought [2].

The documented precipitation decrease in the subtropics during the last 3–4 decades has favored the occurrence of persistent large-scale droughts [3]. Frequent drought events over the Southern Hemisphere subtropics have been mainly attributed to the recent poleward expansion and intensification of the descending branch of the Hadley Circulation [4]. Indeed, widespread droughts have affected recently several regions in the Southern Hemisphere. In South America, an uninterrupted rainfall decline was recorded in Central Chile from 2010 to date [5,6], while the semi-arid northeastern Brazil has experienced since 2010 the longest and most intense drought in decades [7], with more than 10 million people affected and large losses on rainfed agriculture [8]. A period of unprecedented rainfall shortage, called the “Millennium Drought”, has also been registered in Australia [9], at the time that 2015 was the year with the lowest national annual rainfalls since records started in 1904 in South Africa [10].

The arid Central Andes of Argentina (CAA, 31° S–37° S; 67° W–71° W) has also been affected by persistent severe droughts. The Water Administration Department from the Mendoza province (Departamento General de Irrigación) established the hydrological emergency in 2010. This hydrological status for the region continues today (May 2017). The Hydraulic Department from the San Juan province (Departamento de Hidráulica) reported the onset of the hydrological drought in 2009, when streamflow reduction amounted to 40%. Dams and reservoirs faced a marked reduction in water storages with severe consequences for intensive agriculture, the dominant regional activity only possible through irrigation [11]. Being the major wine producer region in Argentina, the agro-industrial activities in CAA depend largely on grape production [12]. Impacts of the 2010–2015 drought also affected the hydropower generation [13] and international tourism [14]. The amount of penalties in relation to water misuse increased in quantity and cost [15,16], in an attempt to optimize the limited water resources by the water administration agencies. To face the increasing severity of drought across the CAA, large-scale grape producers gradually set the new grape production areas at upper elevations by the Andes foothills, looking for lower temperatures, proximity to water sources, better water quality, and less environmental pollution [11]. These geographical changes in areas of grape production have intensified the upstream-downstream water conflicts between producers within basins. At regional scale, conflicts between provincial administrations have also been exacerbated due to the recent dominant drought conditions prevailing in most Central Andes basins during the last decade [17,18].

Climate change will exacerbate the spatial and temporal patterns of meteorological and hydrological droughts, including changes in seasonal distribution of water stress, thereby producing more frequent and more intense droughts with longer duration [1]. In this sense, the knowledge of processes causing hydrological drought and its spatial variability is essential for a sustainable management of water resources [19]. Basins in the CAA have a marked snowmelt-driven hydrological regime, with a runoff peak in the warm season and low flows during winter months [20]. Above normal streamflows occur during El Niño years; however, during La Niña events, the occurrence of low snowfall—i.e., potential hydrological drought conditions—is not straightforward [21]. The hydrological cycle in the CAA is likely to be modified under future climate scenarios with a long-term decrease in streamflow linked to reduced snow accumulation and an early peak in streamflows due to anticipated warmer springs [22,23]. Under future projections, it is crucial to deepen our knowledge on hydrological drought across the region and particularly the associated large impacts.

The objective of this study is to characterize the recent extreme hydrological drought (2010–2015) along the CAA in terms of its onset, spatial extension, mean duration and maximum severity. The assessment of hydrological droughts will be performed through the analysis of streamflow data, a key variable to identify drought events with reference to some specific threshold levels [24]. A comparison of this long-lasting event with previous droughts recorded during the last 46 years will be performed in terms of drought characteristics, its links with snow accumulation and the related atmospheric and oceanic drivers. To further identify the spatial extension of this hydrological

drought, we also included in the assessment some of the major basins from North Patagonia (NP, 37° S–41° S; 68° W–72° W), totalizing 20 rivers located between 31° S and 41° S. Recommendations based on both the need of an adequate streamflow monitoring system and the role of thresholds for drought declaration purposes are also discussed.

2. Materials and Methods

2.1. Data

Monthly streamflow records from 20 stations located between 31° S and 41° S (Figure 1) were retrieved from the hydrological database belonging to the Water Resources Agency of Argentina (<http://bdhi.hidricosargentina.gov.ar/>). Our records included the major rivers from the CAA and NP regions. These stations were selected based on the quality of the data, the spatial representativeness of the stations over the study area and the length of the runoff series. Raw streamflow data were previously subjected to quality control and gap filling routines, as described in [25,26]. Data infilling was minimal since the selected stations have less than 5% missing data. Linear regressions between the selected series and data from neighboring gauge stations were used to complete the data gaps. Following these procedures, the 1971–2016 common period between records was considered to characterize the hydrological droughts, although some records have data until the year 2015. Given that streamflow variability over the CAA is modulated by snowmelt [21,27], snow records, expressed as snow water equivalent between 1989 and 2015, from six stations distributed between 29° S and 37° S were also included in our analysis (Figure 1). Selected stations are summarized in Table 1. It is worth mentioning that, between the headwaters and the location of the stream gauges, there are no major reservoir or dam constructions that can alter the natural flow and, therefore, affect the estimation of streamflow drought occurrences.

Table 1. Geographical information on selected stations. IDs with an asterisk (*) correspond to snow course.

ID	River	Station Name	Lat (° S)	Lon (° W)	Altitude (m a.s.l.)	Mean Streamflow (m ³ /s)
1205	de los Patos	Alvarez Condarco	31.92	69.70	1923	20.6
1211	San Juan	KM 101	31.25	69.18	1310	53.4
1403	Atuel	La Angostura	35.10	68.87	1302	37.5
1407	Cuevas	Punta de Vacas	32.87	69.77	2406	7.2
1413	Mendoza	Guido	32.92	69.24	1408	49.6
1415	Salado	Cañada Ancha	35.20	69.78	1680	11.1
1419	Tunuyán	Valle de Uco	33.78	69.27	1199	28.9
1420	Tupungato	Punta de Vacas	32.88	69.76	2450	24.9
1421	Vacas	Punta de Vacas	32.85	69.76	2400	4.7
1423	Diamante	La Jaula	34.66	69.31	1500	33.8
1425	Poti Malal	Gendarmería	35.87	69.95	1485	7.6
1426	Pincheira	Pincheira	35.51	69.80	1750	5.4
1427	Grande	La Gotera	35.87	69.89	1400	108.2
2001	Barrancas	Barrancas	36.80	69.89	950	38.3
2002	Colorado	Buta Ranquil	37.08	69.75	850	151.3
2004	Neuquen	Paso de Indios	38.53	69.41	498	295.5
2005	Chimehuin	Naciente	39.79	71.21	875	62.6
2010	Agrio	Bajada del Agrio	38.37	70.03	660	79.1
2021	Cuyín Manzano	Cuyín Manzano	40.77	71.18	675	9.9
2040	Quilquihue	Junín de los Andes	40.05	71.10	750	31.2
9250 *	Jachal	Cerro Negro	29.89	69.56	4172	-
9145 *	Mendoza	Toscas	33.16	69.89	3000	-
9131 *	Diamante	Laguna Diamante	34.20	69.70	3301	-
9104 *	Atuel	Laguna Atuel	34.51	70.05	3423	-
9121 *	Grande	Valle Hermoso	35.14	70.20	2253	-
9120 *	Grande	Paso Pehuenches	35.98	70.39	2555	-

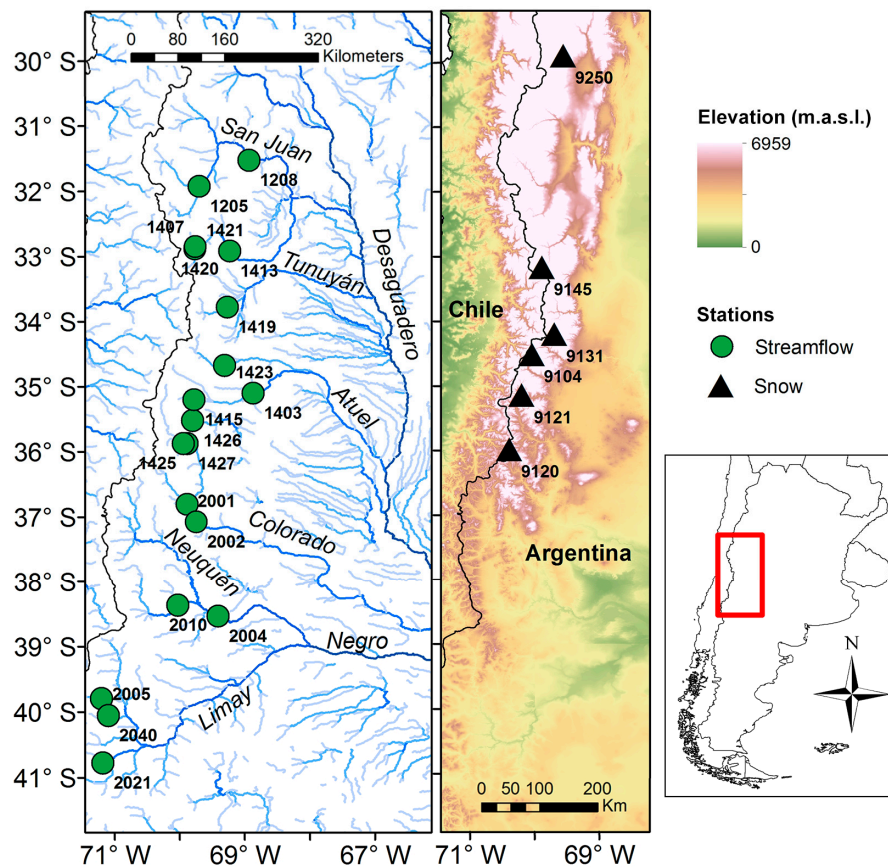


Figure 1. Spatial distribution of the hydrometeorological stations used in this study. The main rivers and the topography of the Central Andes in Argentina are also indicated.

2.2. Hydroclimatic Features

The Andes strongly affect the regional precipitation patterns through interactions with the continental atmospheric circulation and the incursion of moist air masses from the Pacific Ocean [25]. With a mean elevation of 3500 m north of 35° S, the Andes act as a permanent barrier to the humid air masses from the mid-latitude South Pacific Ocean. At high elevations in the Andes, the climate shows a Mediterranean regime with a marked precipitation peak during the cold months (April to October) and little precipitation during the warm summer season (November to March [20]). The precipitation pattern drives the CAA hydrological cycle, exemplified in Figure 2 for the Mendoza River. The annual streamflow cycle was defined as the period between July of year t and June of year $t + 1$. A pronounced streamflow peak during the spring-summer season is associated with snowmelt and glacier melting due to warmer temperatures. At the Mendoza River, the mean monthly streamflow for January exceeds 100 m³/s. In contrast, the low flow season is observed during the cold winter months, with monthly streamflow values close to 20 m³/s (Figure 2). Due to the strong rain shadow effect, climate east of the Andes is arid to semi-arid, with annual precipitation totals ranging between 100 and 400 mm. These totals are mostly associated with summer rainfalls favored by moist air masses from the Amazon and Atlantic basins [28].

South of 35° S, the mean elevation of the Andes decreases to about 1500 m. Along these ranges and adjacent foothills, rainfall is abundant (reduced) during winter (summer) in response to the northward (southward) shift of the South Eastern Pacific High off the Chilean coast [26]. Annual precipitations range from over 1200 mm at the high elevations of the continental divide to less than 300 mm east of the Andes. The annual cycle of the rivers south of 35° S shows two annual maxima, as exemplified for the Agrio River in Figure 2. One streamflow peak is associated with the winter rainfalls (June–July, >100 m³/s) and the second with the snowmelt at higher mountains during spring–early summer (October–November, ~120 m³/s). The annual streamflow cycle for the rivers south of 38° S goes from April of year t to March of year $t + 1$.

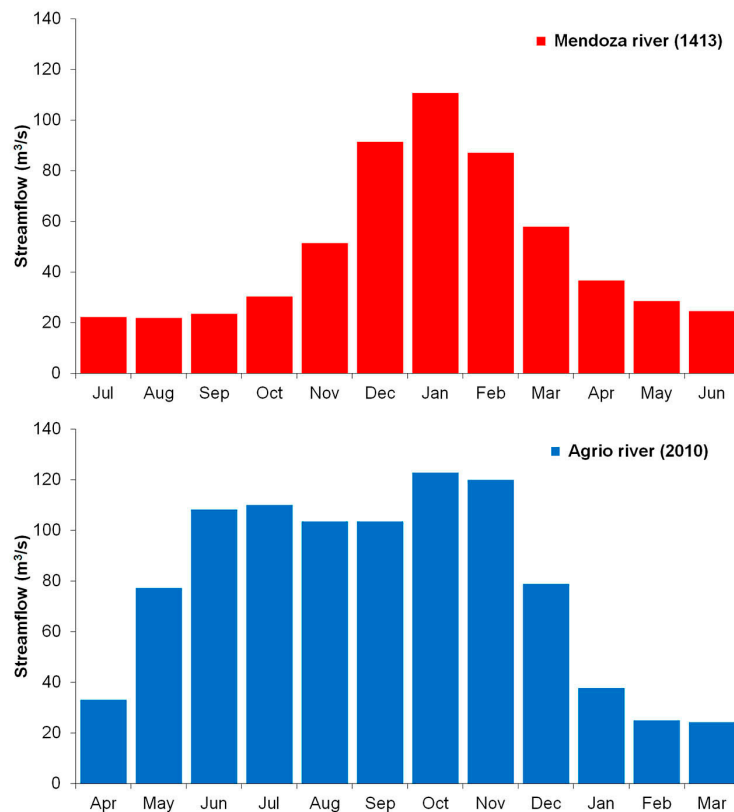


Figure 2. Hydrological cycles from two regional representative basins: the Mendoza River for the Central Andes of Argentina (CAA) and the Agrio River for North Patagonia (NP).

2.3. Methods

Hydrological drought was assessed in terms of streamflow variations, using the standardized streamflow index (SSI, [29]), a widely used index conceived as an extension from the standardized precipitation index (SPI, [30]) to depict hydrologic aspects of droughts. In this sense, the SSI quantifies the number of standard deviations that the streamflow deviates from the climatological mean of a location, by transforming monthly streamflows into z -scores [31]. For the calculation of the SSI, streamflow series were divided in 12 monthly series of 46 years. Each series was fitted to a lognormal probability density function, i.e., the distribution that better fits to streamflow records across the study area [32]. The 12 probability density functions were transformed to the standard normal distribution with mean 0 and variance 1 to finally obtain the SSI time series. A detailed description of the calculation steps for deriving the SSI is provided by Vicente-Serrano et al. [29]. This index was obtained through the SCI package for R [33], a commonly used package to calculate standardized drought indices. In this study, the SSI was calculated on time scale of 3 months (SSI3), following previous work from [34,35]. Nevertheless, the index can be obtained on many time scales (i.e., accumulating streamflow monthly data over 1, 3, 6, 12 or 24 months).

Following the assessment described in [30], the hydrological drought is defined as a period in which the SSI is continuously negative and the index reaches a value of -1.0 or less. The drought begins when the SSI first falls below zero and ends when a positive value of SSI appears, following a value of -1.0 or less. Thus, streamflow departures from average conditions need to exceed one standard deviation. This definition facilitates clear identifications of the onset and the end of the hydrological drought event and determination of other common used statistics such as the drought duration, its magnitude and severity. Three drought categories were used for hydrological drought assessment, based on the categories established for the SPI to define meteorological drought conditions [36]. Table 2 shows the SSI categories, which are in line with recent research based on the SSI [31,32,37,38] and will help to compare the results obtained considering meteorological drought assessment based on the SPI over SSA (e.g., [39]).

Table 2. Standardized streamflow index (SSI) categories.

Category	Index Value
Excess	≥ 1.00
Normal	-0.99 to 0.99
Moderate drought	-1.49 to -1.00
Severe drought	-1.99 to -1.50
Extreme drought	≤ -2.00

3. Results

3.1. The 2010–2015 Hydrological Drought on a Recent Historical Context (1971–2016)

In order to put the 2010–2015 hydrological drought in a historical context, we analyze, over the last 46 years, the variations in the SSI3 for the Mendoza and Agrio Rivers as representative records of CAA and NP, respectively. Figure 3 shows the variations in monthly streamflow and SSI3 for the Mendoza River from July 1971 to June 2016. Based on Figure 3, we observed that above-average streamflows are mainly recorded in the periods 1977–1995 and 2006–2010, whereas below-average streamflows were registered in 1971–1977, 1995–2001 and 2010–2016. Wet and dry periods are not only based on streamflow peaks during the warm season, but also along the annual low flows. For instance, an increase (decrease) in the streamflow during the low-flow season is observed together with an increase (decrease) in the streamflow peaks in summer wet (dry) periods. Regarding the hydrological drought for CAA in the recent period, we noted that severity reached the extreme category between December 2010 and January 2011, being the lowest SSI3 value on record. Even when drought duration seems to be comparable to the event between 1974 and 1977, the number of months with SSI3 values lower than -1.0 is remarkable larger in the most recent drought. When comparing the Mendoza River with the most rivers in the CAA, similar patterns regarding severity, duration and timing of the recent hydrological drought emerge (not shown), consistent with the homogeneous behavior of streamflow variations across the CAA [21,40], and particularly in line with the regionalization performed by [31] based on the SSI for the period 1961–2006.

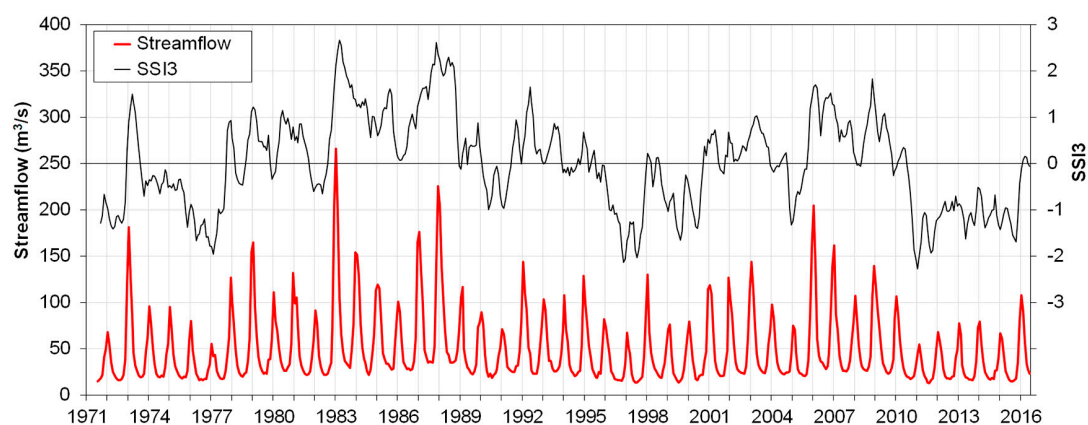


Figure 3. Temporal evolution of monthly streamflow (red line) and monthly SSI3 (black line) for the Mendoza river (1413 station) over the period July 1971–June 2016.

Streamflow and SSI3 variations across NP, based on the records from Agrio River are depicted in Figure 4. Both monthly streamflow and SSI3 records show a more “noisy” pattern in comparison with the Mendoza River (Figure 3). This result is consistent with Caragunis et al. [41], who showed that the contribution of low frequency variations to the streamflow variability accounts for 40% and ~15% of the total variance across the CAA and NP, respectively. Main wet periods are observed during the period 1979–1983, whereas hydrological droughts are identified in 1996, 1999 and 2013 (Figure 4). Comparing with records from CAA, there are several differences in timing, duration and occurrence of the maximum severity during the recent hydrological drought. Several drought events

were recorded since 2007, with the maximum severities between 2012 and 2014 (Figure 4). This latter hydrological drought event shows the lowest SSI3 for the Agrio River record, and is comparable in duration and magnitude with the droughts of 1996/1997 and 1998/1999. Analyzing the spatial pattern of the recent hydrological drought across NP, we noted that most basins experienced extreme hydrological droughts between 2012 and 2013, with durations ranging from seven to over 24 months. The extreme hydrological drought in 1998/1999 shows the lowest SSI3 value on record in three of the five basins south of 38° S.

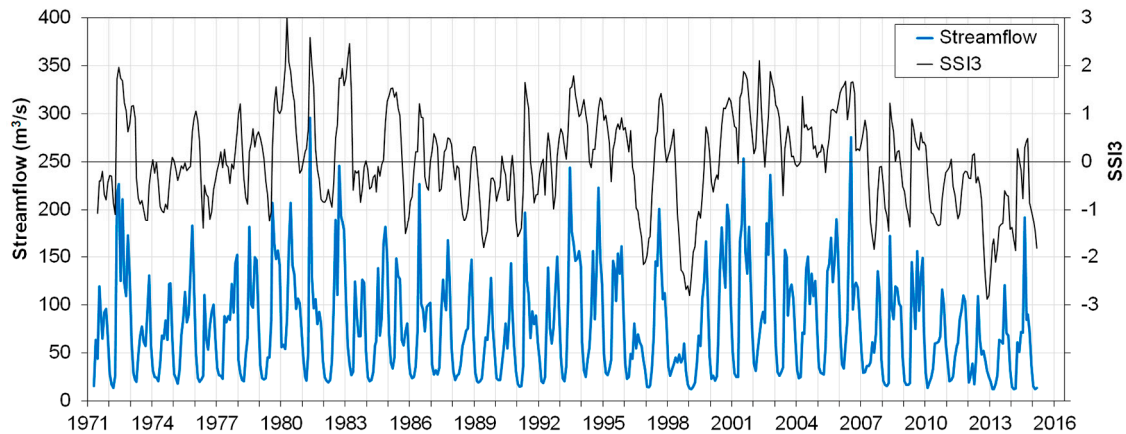


Figure 4. Temporal evolution of monthly streamflow (red line) and monthly SSI3 (black line) for the Agrio river (2010 station) over the period July 1971–June 2016.

Visual inspection of the SSI3 series for each of the selected rivers indicate that, in the basins of NP, the timing of the maximum severity of the 2010–2015 hydrological drought, its duration, onset and demise were not consistent with those recorded for the drought across the CAA (Figures 3 and 4). The spatial representativeness of the 2010–2015 hydrological drought is limited to the basins located north of 38° S. Nevertheless, the intensification of hydrological drought over NP during 2012/2013 is associated with the same physical mechanisms that sustained the drought conditions over the CAA. Details on this aspect are provided in next sections.

The percentage of stations within each SSI3 category is useful to quantify the spatial extension of drought events, even when it is limited by the lack of information in the immediate surroundings. Nevertheless, streamflow integrates the hydrological processes over a river basin and the selected stations belong to similar and spatially contiguous basins over the study area, i.e. providing an acceptable estimation of the proportion of area under drought conditions. The temporal evolution of this index, represented in Figure 5, was obtained for each month during the period 1971–2016 by calculating the percentage of stations with SSI3 below the selected thresholds (see Table 2). The percentage of stations in the moderate drought category includes those stations showing severe and extreme drought conditions. Likewise, the percentage of stations in the severe category includes those stations showing extreme drought. We used the percentage of stations instead of the number of stations given the length differences in the records between CAA and NP regions, particularly after 2015. In general, regional hydrological droughts are observed during 1976/1977, 1991/1992, 1996/1997, 1998/2000 and 2010–2016, with more than 50% of the study area under hydrological drought conditions at different severity levels (Figure 5). During December 1996, January 1997 and between July and October 2015, all the analyzed rivers show hydrological droughts at different severity levels. The 2010–2015 hydrological drought is substantially longer than any other drought event in the last 46 years. On average, between April 2010 and December 2015 (69 months), 63% of the rivers along the study area were affected by moderate to extreme streamflow drought conditions. In terms of severity, however, the droughts of 1996/1997 and 1999/2000 affected a larger percentage of stations under extreme dry conditions, although with shorter durations.

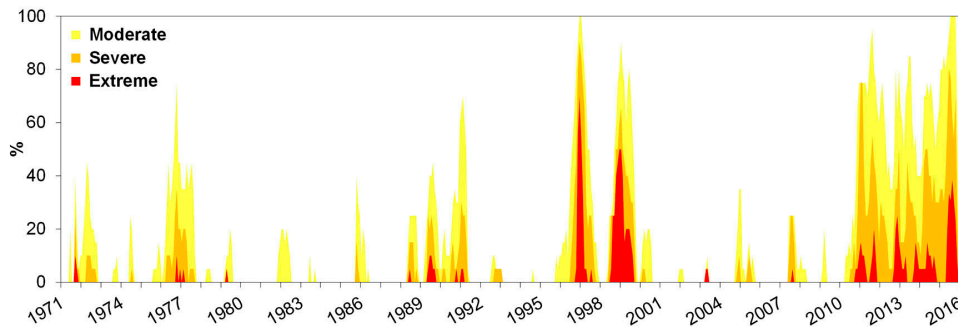


Figure 5. Temporal evolution of the percentage of stations in the Central Andes of Argentina and North Patagonia with hydrological droughts during 1971–2016. Yellow, orange, and red colors indicate moderate, severe, and extreme drought conditions, respectively.

In terms of severity and spatial extension, three of the most important hydrological droughts over the last 46 years were recorded in 1996/1997, 1999/2000 and 2010–2015 (Figure 5). To compare the spatial extension of these droughts during the month showing the maximum intensity, Figure 6 displays the regional patterns of the hydrological drought categories for these three events. As expected from Figure 5, the worst conditions in terms of severity and extension are registered during December 1996, with all the records under drought conditions, 18 reaching the severe category and 14 under extreme hydrological drought conditions. The spatial extension of the hydrological drought during January 1999 seems to be limited to the stations south of 33° S, although the two stations with normal conditions have negative SSI3 almost reaching the moderate category. In a regional perspective, [31] showed that this drought event extended farther south, affecting the basins in Central Patagonia reaching 45° S. During August 2015, only 13 stations located across the CAA have available records. All rivers were under moderate hydrological drought, eight and five of them reaching the severe and extreme drought categories, respectively. Hydrological drought severity exhibits a more heterogeneous pattern, attributed by Rivera et al. [25] to geomorphological factors within each basin. However, additional studies are needed to properly account for the difference between basins.

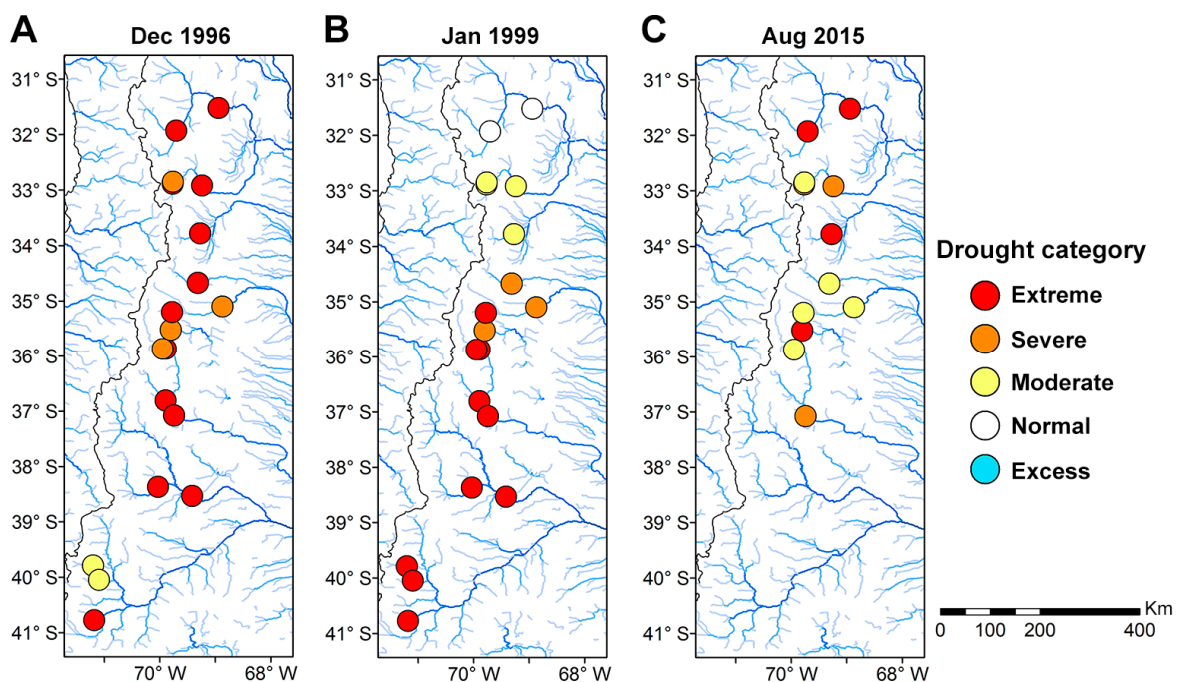


Figure 6. Spatial distribution patterns for the hydrological droughts according to drought categories during: December 1996 (A); January 1999 (B); and August 2015 (C). No data are available for the NP gauges during August 2015.

3.2. Spatial and Temporal Patterns of the 2010–2015 Hydrological Drought

For assessing the spatial and temporal patterns of the 2010–2015 hydrological drought, 15 stations from the CAA were analyzed. SSI3s from July 2009 to June 2016 are shown in Figure 7. In most gauges, the onset of the hydrological drought started during the second half of 2010. SSI3s rapidly fall below -1.0 , with extreme droughts in the Mendoza, Tupungato and Vacas Rivers during the summer of 2011 and severe drought conditions in the rest of the rivers in the CAA. Across the CAA the 2010–2015 hydrological drought is a continuous, long-lasting event. Only three stations recorded SSI3 positive values in October 2012 (Diamante River), October–November 2013 (Grande River) and November 2013 (Barrancas River). Three peaks in drought intensity are evident: the first between 2010 and 2012, the second between 2014 and 2015 and the last between 2015 and 2016. Stations reaching extreme hydrological droughts during the first intensity peak are located between 32° S and 34° S, whereas those related to the second intensity peak between 34° S and 37° S. A more heterogeneous spatial pattern is observed for the 2015–2016 intensity peak, as represented in Figure 6. The hydrological drought demise is recorded between the end of year 2015 and the beginning of 2016, although some stations continued under hydrological drought conditions (i.e., Tunuyán, Vacas, Poti Malal and Pincheira, see Table 1 for more details).

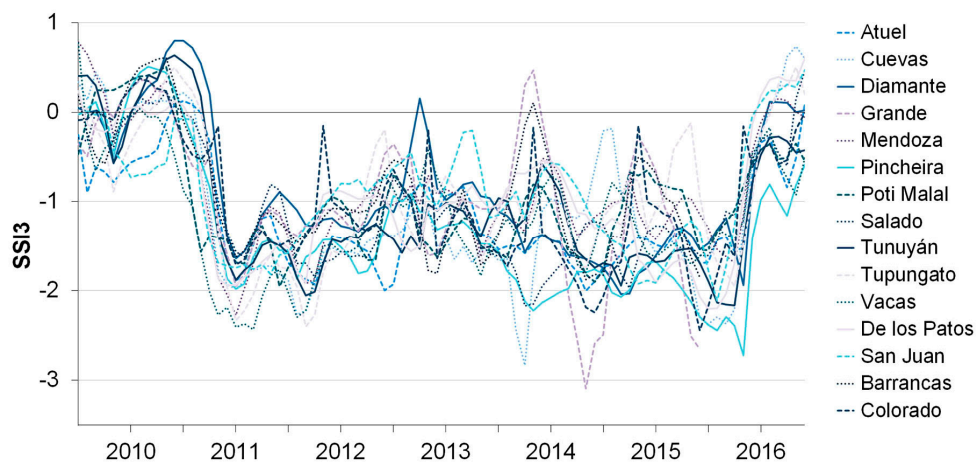


Figure 7. SSI3 evolution from July 2009 to June 2016 for the 15 stations located across the Central Andes of Argentina.

The spatial distribution of the hydrological drought severity at different stages during the 2010–2015 drought event is shown in Figure 8 for the months of January, May and September in the years 2011 to 2015. As previously recorded for the temporal variability in SSI3, differences in drought spatial patterns arise from the comparison between the CAA and NP rivers. Less intense drought severities are observed over the NP basins, except for the period between September 2012 and May 2013. As shown in Figure 7, the hydrological drought develops and intensifies quickly, with severe drought conditions in all CAA basins during January 2011. The hydrological drought event across the CAA decreases in severity since January 2012, with few stations showing moderate drought conditions in September 2012 and January 2013. This spatial pattern contrasts with the increase in severity over NP, suggesting that the intensification of drought could be related to reduced rainfalls south of 38° S. Over the period 2010–2015, higher drought severity was recorded in rivers located between 35° S and 36° S. Water demand for irrigation in the CAA is larger during spring-summer months; therefore, when comparing the hydrological drought categories during January it can be seen that the large number of stations under drought was observed during 2011 and 2015. This result is in line with drought intensity peaks in Figure 7.

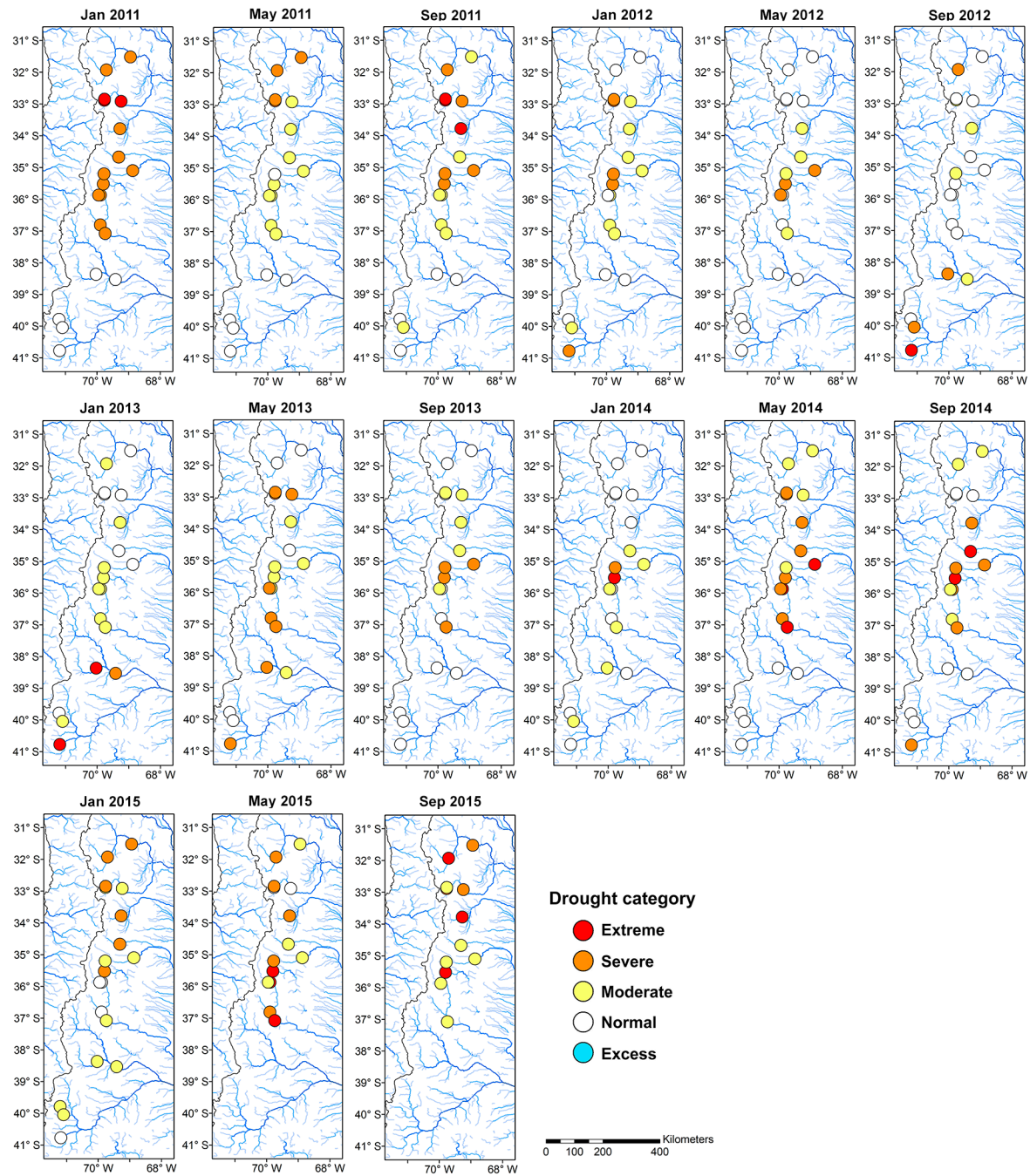


Figure 8. Spatial distribution of hydrological droughts by categories during January, May and September from 2011 to 2015.

Table 3 summarizes the main hydrological drought characteristics over the period 2010–2016. Except for the San Juan River, the remaining gauges show that the onset of the hydrological drought occurred between June and October 2010. The drought ended during the first part of 2016, although four rivers still remain under drought conditions at the end of the records. The mean hydrological drought duration was 67 months, being one of the longest dry periods in the CAA rivers. Six rivers registered the lowest SSI3 values (i.e., maximum drought severity) of the entire record (1971–2016). A large heterogeneity is observed in the date of the maximum hydrological drought severity, consistent with the findings on meteorological drought conditions reported by [42,43].

Table 3. Characteristics of the 2010–2015 hydrological drought.

ID	River	Onset	Demise	Duration (Months)	Maximum Severity
1205	de los Patos	August 2010	January 2016	65	−2.20 (July 2015)
1211	San Juan	November 2009	January 2016	74	−2.11 (August 2015)
1403	Atuel	October 2010	June 2016	68	−2.01 (May 2014) *
1407	Cuevas	September 2010	February 2016	65	−2.83 (October 2013) *
1413	Mendoza	July 2010	February 2016	67	−2.28 (January 2011) *
1415	Salado	July 2010	May 2016	70	−2.17 (October 2013)
1419	Tunuyán	October 2010	-	69	−2.17 (October 2015)
1420	Tupungato	October 2010	March 2016	65	−2.40 (September 2011) *
1421	Vacas	March 2010	-	76	−2.44 (March 2011) *
1423	Diamante	November 2010	February 2016	23 + 39 ***	−2.04 (September 2014)
1425	Poti Malal	July 2010	-	72	−1.95 (June 2011)
1426	Pincheira	July 2010	-	72	−2.72 (November 2015) *
1427	Grande	June 2010	June 2015 **	40 + 19 ***	−3.09 (May 2014)
2001	Barrancas	July 2010	June 2015 **	40 + 19 ***	−1.88 (May 2014)
2002	Colorado	June 2010	June 2016	72	−2.45 (June 2015)

Notes: * indicates that the maximum severity during the recent drought was the lowest SSI3 value over the period 1971–2016. ** indicates the last date of the streamflow records. *** indicates that two drought events were recorded between 2010 and 2015, although the period with positive SSI3 values was shorter than 3 months, suggesting that the two drought events could be merge in a single drought.

3.3. Drivers of the Hydrological Drought

Since hydrological drought conditions over the CAA respond to lower than average accumulation of snow over the Andes [21,44], we explore the relationship between drought and the mean regional snow water equivalent anomaly (SWEA) over the period 1989–2015. The annual (July to June across the CAA) percentage of stations with hydrological drought conditions highlights the strong link between large negative (positive) anomalies in SWEA and the occurrences of widespread hydrological droughts (excesses; $r = 0.67$, $p < 0.01$; Figure 9). The largest negative anomalies in SWEA were registered in 1996 and 1998, leading to severe to extreme hydrological drought conditions over most of the CAA basins (Figures 5 and 6). A dry pattern was also observed over NP in those years (see Figures 4 and 5), but the small contribution of rainfall, instead of snow, likely is the main driver. The 2010–2015 drought was entirely consistent with six years in a row showing negative SWEA anomalies (Figure 9) and a mean of 68% of the basins affected by drought between 2010/2011 and 2015/2016. Positive SWEA leads to a lower percentage of stations showing droughts (Figure 9).

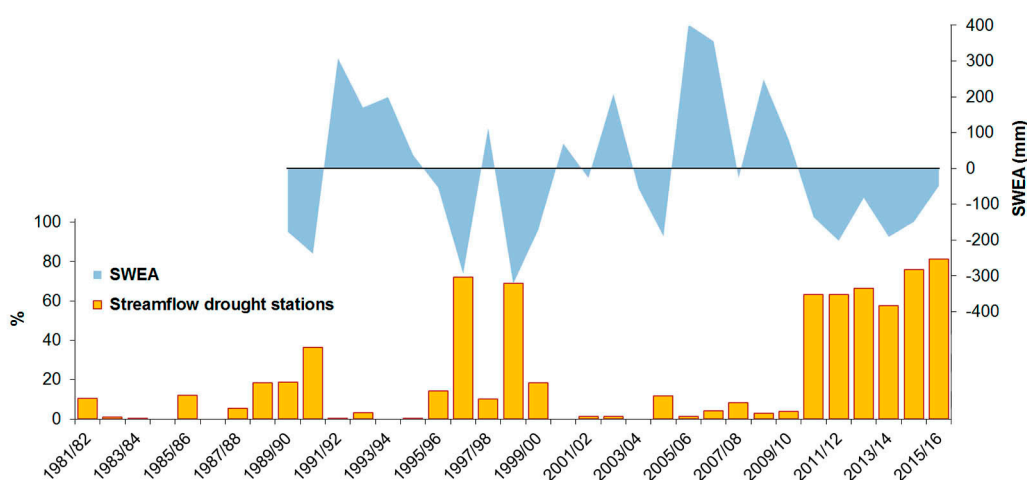


Figure 9. Temporal evolution of mean regional snow water equivalent anomalies (SWEA; 1989–2015) and mean annual (July to June) percentage of stations showing hydrological droughts (1981/1982 to 2015/2016).

Previous research shows that La Niña events are related to lower than average snow accumulation over the CAA [21]. The sea surface temperature (SST) anomaly field for the months with at least 70% of the gauges recording hydrological droughts is shown in Figure 10 for the period 1989–2014. A clear La Niña pattern is evident over the tropical Pacific Ocean, with cold SST over the equatorial ocean. This pattern emerges after discarding the year 2015, which recorded a very strong El Niño event. Warm SSTs over the subtropical Pacific Ocean east of Australia are produced by the advection of warm water from the tropics toward the subtropics (Figure 10). Based on the Oceanic Niño Index (see [45] for details), we noted that the years 2010/2011 and 2011/2012 were classified as La Niña years, while 2012/2013 and 2013/2014 also characterized by cold SSTs over the tropical Pacific Ocean not reached La Niña threshold. Including the year 2015, anomalies over the tropical Pacific Ocean still remain below zero, whereas the warm region in the subtropics show similar anomalous values (not shown).

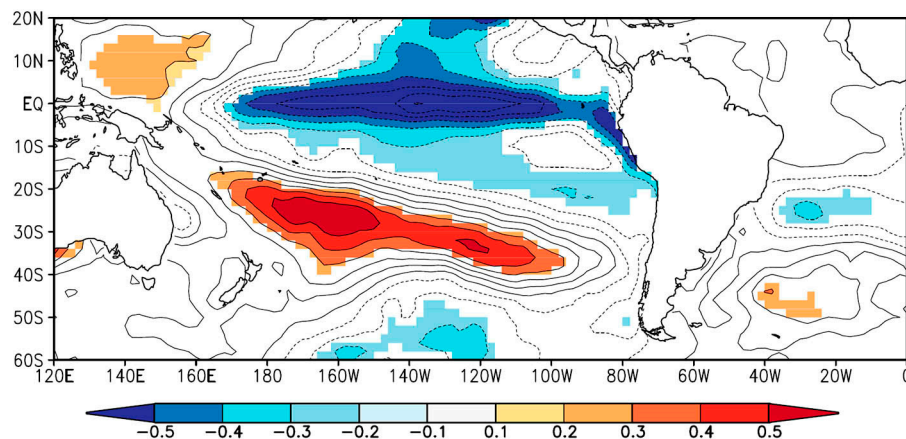


Figure 10. Composite of SST (Extended Reconstructed Sea Surface Temperature v3b, [46]) anomalies (1989–2014) during the months showing more than 70% of the stations with hydrological drought conditions. Color areas are significant at the 95% significance level.

Figure 11 shows the composite anomaly for the 500 hPa geopotential height (Z500) during the same months used for developing the SST anomaly composite. Figure 11 displays a strengthening and southward latitudinal location of the semi-permanent south Pacific subtropical anticyclone. This circulation pattern is associated with a decrease of the westerly zonal winds at subtropical latitudes and the decrease of the frontal activity over the study area.

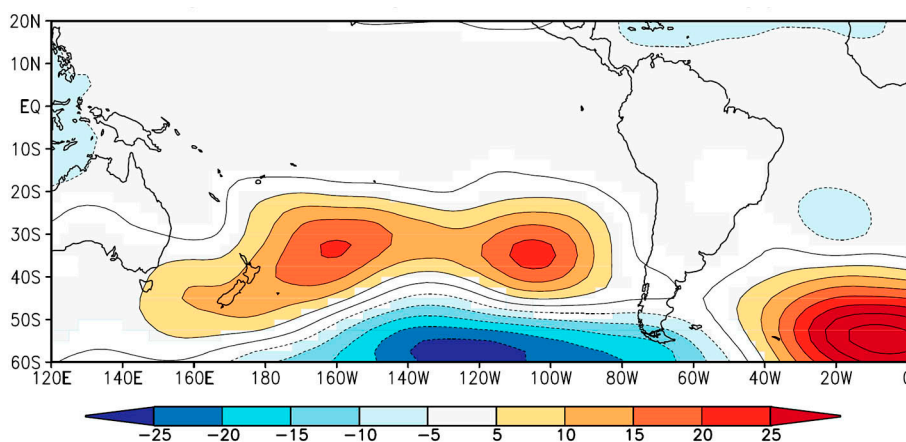


Figure 11. Composite of Z500 (NCEP/NCAR Reanalysis, [47]) anomalies (1989–2014) during the months showing more than 70% of the stations with hydrological drought conditions. Color areas are significant at the 95% significance level.

4. Discussion

The period of persistent below-average snow accumulation over the Central Andes between the years 2009 and 2015 was remarkably anomalous over the last 27 years and significantly reduced the snow contribution to discharge for the major rivers along the adjacent Chilean and Argentinean territories. These rivers sustain the agricultural oases that fed almost 2.5 million inhabitants along the CAA adjacent lands [25]. Therefore, understanding the hydrological drought variability and forcings, as well as the associated impacts to human and ecosystems is a key aspect for water management over the semi-arid CAA. In this sense, the term “snow drought” is gaining traction in the scientific community [48,49], a condition that refers to the combination of general drought and reduced snow storage. Snow drought is not a new hazard across the CAA, we just need to look at the snowpack records from the years 1968 or 1996 to verify that is a recurrent phenomenon commonly linked to meteorological drought conditions over central Chile (see [50] for example). Nevertheless, climate change and climate variability on interannual and interdecadal time scales added new facets to snow droughts, which motivated the definition of dry snow drought—accounting for the lack of precipitation—and warm snow drought—condition where temperatures prevent precipitation from accumulating on the landscape as a snowpack [48]. Further studies are needed to clarify its contribution to the hydrological drought across the CAA. Moreover, several other factors need to be addressed to fully understand the hydrological cycle in the region, as for example the glacier melt contribution during drought periods, the groundwater dynamics or the losses of snow due to sublimation processes. Ground observations are limited across the CAA, highlighting the need to use remote sensing products or modeled hydrometeorological data to address these challenges.

Streamflow data were used as a key variable that synthetize the hydrological processes to define hydrological droughts. Even when this kind of drought involves several components of the hydrological cycle, such as snow, groundwater and reservoir and lake levels, streamflow variations were able to depict the main hydrological drought periods across the CAA. Using the SSI [51], found a significant link between streamflow from the main rivers across the CAA and Llanquihue lake areal averages, the major water body in the region. A decrease of 41.6% in the surface of the lake was observed between October and November 2010 [51], in line with the sharp decrease in the SSI3 across the CAA (Figure 7). Moreover, the years 2010–2013 are the longest period of sustained small lake size in the period 1984–2013 [51]. The results from our study support the homogeneous behavior of streamflow and hydrological droughts, considering the differences observed between the spatial and temporal variations of the NP basins during the 2010–2015 drought period.

The use of the standardized indices for drought characterization is increasing steadily, in line with the needs of monitoring of different hydrological variables across several climatic regions. In Argentina, several agencies as the National Weather Service and the National Institute of Agricultural Technology use the SPI for meteorological drought monitoring and assessment. In this sense, it is expected that the outcomes from the SSI can be easily interpreted by meteorological and hydrological agencies, water managers and scientists focused on drought research and monitoring [31]. One of the main advantages of using the SSI is its flexibility when contrasting hydrological regimes and flow characteristics are involved [52], allowing the comparison among different regions and basins regardless of streamflow magnitudes [53]. We believe that the SSI has the potential to improve hydrological drought monitoring across the CAA and NP and might be integrated with the actual streamflow monitoring, which is based on the percentage of normal streamflow. The effect of multidecadal climate variability limits the applicability of the SSI, as shown by [35]. Nevertheless, this study attempted to limit this negative effect by selecting only 46 years of data. In this sense, water agencies can declare hydrological drought conditions with a minimum of 30 years of data, a period of records that can allow a good density of gauges across the CAA. For hydrological drought declaration, thresholds are a fundamental piece. In this work, the streamflow drought categories (Table 1) were selected based on the thresholds typically used to define meteorological droughts based on the SPI. This operational definition can diverge from the conceptual or political definitions of hydrological drought [35]. For example, categories as mild drought can be used to have a better picture than the wide “normal” category, which covers 68% of the SSI variability. This limitation was

observed in Figure 6, in which the rivers of San Juan province were under normal conditions but the SSI3 value was close to -1.0 .

Long-term trends in streamflows across the CAA are highly dependent on the period considered for the analysis, as shown by [21,54,55] among others. Recent negative trends in snow cover extent during 1979–2014 were mainly attributed to changes between 3000 and 5000 m a.s.l. [56], and can be responsible for the recent trends in streamflow across the CAA. Further studies are needed to properly quantify the role of the Pacific Decadal Oscillation (PDO) in the 2010–2015 hydrological drought, considering longer streamflow records to adequately represent the interdecadal variability. A strong non-linearity in the behavior of long-term trends was observed considering the seasonal number of days with low flows [25], linked to the decadal behavior of the PDO. The cold (warm) phase of the PDO is linked to below (above)—average winter snowpacks and annual discharges [25,57]. Nevertheless, Boisier et al. [5] have shown that the PDO accounts for half of the recent precipitation trends recorded in the Central Andes. This negative trend in precipitation reconciles with model results only if the anthropogenic forcing and the observed SST changes are accounted for jointly. When considering future changes in the hydroclimatology of the Central Andes, the region is likely to become drier and warmer in response to anthropogenic climate change [22,23,58–60], with an increase in meteorological drought frequency and severity [42]. These projected changes will likely change the characteristics of future hydrological drought across the CAA, an assessment that needs to be performed to assist adaptation strategies.

5. Conclusions

The 2010–2015 hydrological drought across the semi-arid CAA and NP regions was assessed in terms of streamflow variations through the SSI3. The main characteristics of this dry episode—spatial distribution, temporal evolution, and timing of severity—indicate that its spatial extension was limited to the basins north of 38° S. This result prevents concluding that the recent hydrological drought affected in a similar way the CAA and NP. The northern extension is limited due to the data availability until 31° S, but an assessment of the drought event affecting Central Chile [6] showed similar drought conditions as north as 28° S. In this sense, the core region was the CAA, where snow accumulation plays a relevant role in the streamflow amount and timing. In a regional perspective, 68% of the CAA basins were continuously affected by hydrological drought from moderate to extreme severity between 2010 and 2016. The mean duration of hydrological drought was 67 months—i.e., five years and seven months—standing out as the longest drought period of the record (1971–2016). Moreover, the temporal consistency of the drought event is comparable on the long-term context with the drought of 1967/1968 to 1971/1972 [61]. Taking into account population growth, impacts of the recent hydrological drought could be stronger than the recorded during the period 1967/1968 to 1971/1972.

We need to point out that four of the analyzed rivers continued under hydrological drought until the end of our records (June 2016), but with SSI3 values close to zero. Six of the rivers recorded the lowest SSI3 value during the 2010–2015 drought, with 14 out of 15 stations reaching the extreme category. The role of snow accumulation was assessed through the SWEA, identifying that the regional hydrological droughts were associated to lower than normal snow accumulation over the Central Andes. This feature is likely to be linked to La Niña pattern, with cold SSTs over the tropical Pacific Ocean and positive anomalies in the subtropical Pacific east of Australia. This oceanic forcing generated a rainfall shortage that contributed to almost 100 days with low flows in the basins of NP between 2012 and 2013 [26], a factor that was observed through severe hydrological drought conditions mainly between September 2012 and May 2013. Nevertheless, even when El Niño–Southern Oscillation seems to be one of the main forcings on hydrological drought variability over the CAA and NP, a lack of spatio-temporal consistency in the 2010–2015 drought was observed, indicating that other factors could be playing a relevant role in the spatial extension of hydrological drought and its severity. Further studies are needed to clarify this issue.

Acknowledgments: This work was carried out with the aid of the following projects: UBACyT 20020130100263BA from the University of Buenos Aires (UBA) and PIP0137 from the National Research Council of Argentina (CONICET). We thank the Subsecretaría de Recursos Hídricos de Argentina for providing the snow and streamflow records used in the study.

Author Contributions: J.A.R. came up with the concept for the manuscript, conducted the analysis and wrote the manuscript with the inputs from all co-authors (O.C.P., R.V. and D.C.A.).

Conflicts of Interest: The authors declare no conflict of interest.

References

- Schwabe, K.; Albiac, J.; Andreu, J.; Ayers, J.; Caiola, N.; Hayman, P.; Ibanez, C. Summaries and Considerations. In *Drought in Arid and Semi-Arid Regions*; Schwabe, K., Albiac, J., Connor, J.D., Hassan, R.M., Meza-González, L., Eds.; Springer: Dordrecht, The Netherlands, 2013; pp. 471–507.
- Tallaksen, L.M.; Van Lanen, H.A.J. *Hydrological Drought: Processes and Estimation Methods for Streamflow and Groundwater*; Elsevier: Amsterdam, The Netherlands, 2004.
- Dai, A. Drought under global warming: A review. *WIREs Clim. Chang.* **2011**, *2*, 45–65, doi:10.1002/wcc.81.
- Cai, W.; Cowan, T.; Thatcher, M. Rainfall reductions over Southern Hemisphere semi-arid regions: The role of subtropical dry zone expansion. *Sci. Rep.* **2012**, *2*, 702, doi:10.1038/srep00702.
- Boisier, J.P.; Rondanelli, R.; Garreaud, R.D.; Muñoz, F. Anthropogenic and natural contributions to the Southeast Pacific precipitation decline and recent megadrought in central Chile. *Geophys. Res. Lett.* **2016**, *43*, 413–421, doi:10.1002/2015GL067265.
- Garreaud, R.; Alvarez-Garreton, C.; Barichivich, J.; Boisier, J.P.; Christie, D.; Galleguillos, M.; LeQuesne, C.; McPhee, J.; Zambrano-Bigiarini, M. The 2010–2015 mega drought in Central Chile: Impacts on regional hydroclimate and vegetation. *Hydrol. Earth Syst. Sci. Discuss.* **2017**, doi:10.5194/hess-2017-191.
- Marengo, J.A.; Alvala, R.S.; Moraes, O.L.; Brito, S.; Cunha, A.P. The 2010–2016 drought in the semiarid Northeast Brazil region: Monitoring, climatic features and socio-economic impacts. In Proceedings of the Multihazard Early Warning Conference, Cancún, México, 22–23 May 2017.
- Paredes-Trejo, F.; Barbosa, H. Evaluation of the SMOS-Derived Soil Water Deficit Index as Agricultural Drought Index in Northeast of Brazil. *Water* **2017**, *9*, 377, doi:10.3390/w9060377.
- Van Dijk, A.I.J.M.; Beck, H.E.; Crosbie, R.S.; De Jeu, R.A.M.; Liu, Y.Y.; Podger, G.M.; Timbal, B.; Viney, N.R. The Millennium drought in southeast Australia (2001–2009): Natural and human causes and implications for water resources, ecosystems, economy, and society. *Water Resour. Res.* **2013**, *49*, 1040–1057, doi:10.1002/wrcr.20123.
- Bureau for Food and Agricultural Policy. *Policy Brief on the 2015/2016 Drought*; BFAP: Cape Town, South Africa, 2016.
- Montaña, E.; Diaz, H.P.; Hurlbert, M. Development, local livelihoods, and vulnerabilities to global environmental change in the South American Dry Andes. *Reg. Environ. Chang.* **2016**, *16*, 2215–2228, doi:10.1007/s10113-015-0888-9.
- Agosta, E.A.; Cavagnaro, M. Variaciones interanuales de la precipitación de verano y el rendimiento del cultivo de la vid en Mendoza. *Geoacta* **2010**, *35*, 1–10.
- Villatoro, G. Cortocircuitos por la creciente crisis hídrica del río Atuel. *Diario Uno*, 25 January 2015. Available online: <http://www.diariouno.com.ar/pais/cortocircuitos-la-creciente-crisis-hidrica-del-ri-atuel-20150118-n43593.html> (accessed on 26 May 2017).
- Romanello, C. Por la sequía, el turismo en el dique Ullum es cada vez menor. *Diario Los Andes*, 19 March 2015. Available online: <http://www.losandes.com.ar/noticia/por-la-sequia-el-turismo-en-el-dique-ullum-es-cada-vez-menor-838737> (accessed on 26 May 2017).
- Diario Los Andes. En sólo 11 días se hicieron 470 multas por derroche de agua en Mendoza. *Diario Los Andes*, 13 November 2014. Available online: <http://www.losandes.com.ar/article/en-solo-11-dias-se-hicieron-470-multas-por-derroche-de-agua-en-mendoza> (accessed on 26 May 2017).
- Diario Uno. Aumentó el valor de las multas por derrochar agua: Las más caras serán de \$5.700. *Diario Uno*, 20 March 2017. Available online: <http://www.diariouno.com.ar/mendoza/aumento-el-valor-las-multas-derrochar-agua-las-mas-caras-seran-5700-20170320-n1361153.html> (accessed on 26 May 2017).
- McIntyre, O. *Environmental Protection of International Water Courses under International Law*; Ashgate Publishing Limited: Hampshire, UK, 2007.

18. Rojas, F.; Wagner, L. Conflicto por la apropiación del río Atuel entre Mendoza y La Pampa (Argentina). *HALAC* **2016**, *6*, 278–297.
19. Nikbakht, J.; Tabari, H.; Hosseinzadeh Talaei, P. Streamflow drought severity analysis by percent of normal index (PNI) in northwest Iran. *Theor. Appl. Climatol.* **2013**, *112*, 565–573, doi:10.1007/s00704-012-0750-7.
20. Masiokas, M.H.; Christie, D.C.; Le Quesne, C.; Pitte, P.; Ruiz, L.; Villalba, R.; Luckman, B.H.; Berthier, E.; Nussbaumer, S.U.; González-Reyes, A.; et al. Reconstructing the annual mass balance of the Echaurren Norte glacier (Central Andes, 33.5 S) using local and regional hydroclimatic data. *Cryosphere* **2016**, *10*, 927–940, doi:10.5194/tc-10-927-2016.
21. Masiokas, M.; Villalba, R.; Luckman, B.; Le Quesne, C.; Aravena, J.C. Snowpack variations in the Central Andes of Argentina and Chile, 1951–2005: Large-scale atmospheric influences and implications for water resources in the region. *J. Clim.* **2006**, *19*, 6334–6352, doi:10.1175/JCLI3969.1.
22. Boninsegna, J.; Villalba, R. Los escenarios de Cambio Climático y el impacto en los caudales. In *Documento Sobre la Oferta Hídrica en los Oasis de Riego de Mendoza y San Juan en Escenarios de Cambio Climático*; Secretaría de Ambiente y Desarrollo Sustentable: Buenos Aires, Argentina, 2006.
23. Villalba, R.; Boninsegna, J.A.; Masiokas, M.H.; Cara, L.; Salomón, M.; Pozzoli, J. Cambio climático y recursos hídricos. El caso de las tierras secas del oeste argentino. *Ciencia Hoy* **2016**, *25*, 48–55.
24. Jain, V.K.; Jain, M.K.; Pandey, R.P. Effect of the Length of the Streamflow Record on Truncation Level for Assessment of Streamflow Drought Characteristics. *J. Hydrol. Eng.* **2014**, *19*, 1361–1373, doi:10.1061/(ASCE)HE.1943-5584.0000922.
25. Rivera, J.A.; Araneo, D.C.; Penalba, O.C. Threshold level approach for streamflow droughts analysis in the Central Andes of Argentina: A climatological assessment. *Hydrol. Sci. J.* **2017**, doi:10.1080/02626667.2017.1367095.
26. Rivera, J.A.; Araneo, D.C.; Penalba, O.C.; Villalba, R. Regional aspects of streamflow droughts in the Andean rivers of Patagonia, Argentina. Links with large-scale climatic oscillations. *Hydrol. Res.* **2017**, doi:10.2166/nh.2017.207.
27. Araneo, D.; Villalba, R. Variability in the annual cycle of the Río Atuel streamflows and its relationship with tropospheric circulation. *Int. J. Climatol.* **2015**, *35*, 2948–2967, doi:10.1002/joc.4185.
28. Schwerdtfeger, W. The atmospheric circulation over Central and South America. In *Climates of Central and South America*; Schwerdtfeger, W., Ed.; Elsevier: New York, NY, USA, 1976; Volume 2, pp. 2–12.
29. Vicente-Serrano, S.M.; López-Moreno, J.I.; Beguería, S.; Lorenzo-Lacruz, J.; Azorin-Molina, C.; Morán-Tejada, E. Accurate computation of a streamflow drought index. *J. Hydrol. Eng.* **2012**, *17*, 318–332, doi:10.1061/(ASCE)HE.1943-5584.0000433.
30. McKee, T.B.; Doesken, N.J.; Kleist, J. The relationship of drought frequency and duration to time scales. In *Proceedings of the Eight Conference on Applied Climatology, Anaheim, CA, USA, 17–23 January 1993*; American Meteorological Society: Boston, MA, USA, 1993; pp. 179–184.
31. Rivera, J.A.; Penalba, O.C. Spatio-temporal assessment of streamflow droughts over Southern South America: 1961–2006. *Theor. Appl. Climatol.* **2017**, 1–13, doi:10.1007/s00704-017-2243-1.
32. Rivera, J.A.; Penalba, O.C. Distribución de probabilidades de los caudales mensuales en las regiones de Cuyo y Patagonia (Argentina). Aplicación al monitoreo de sequías hidrológicas. *Meteorológica* **2017**, in press.
33. Gudmundsson, L.; Stagge, J.H. *SCI: Standardized Climate Indices such as SPI, SRI or SPEI*; R Package Version 1.0-2; ETH: Zurich, Switzerland, 2016.
34. Shukla, S.; Wood, A.W. Use of a standardized runoff index for characterizing hydrologic drought. *Geophys. Res. Lett.* **2008**, *35*, L02405, doi:10.1029/2007GL032487.
35. Núñez, J.; Rivera, D.; Oyarzún, R.; Arumí, J.L. On the use of Standardized Drought Indices under decadal climate variability: Critical assessment and drought policy implications. *J. Hydrol.* **2014**, *517*, 458–470, doi:10.1016/j.jhydrol.2014.05.038.
36. Lloyd-Hughes, B.; Saunders, M.A. A drought climatology for Europe. *Int. J. Climatol.* **2002**, *22*, 1571–1592, doi:10.1002/joc.846.
37. Barker, L.J.; Hannaford, J.; Chiveron, A.; Svensson, C. From meteorological to hydrological drought using standardised indicators. *Hydrol. Earth Syst. Sci.* **2016**, *20*, 2483–2505, doi:10.5194/hess-20-2483-2016.

38. Rangecroft, S.; Van Loon, A.F.; Maureira, H.; Verbist, K.; Hannah, D.M. Multi-method assessment of reservoir effects on hydrological droughts in an arid region. *Earth Syst. Dyn. Discuss.* **2016**, doi:10.5194/esd-2016-57.
39. Penalba, O.C.; Rivera, J.A. Precipitation response to El Niño/La Niña events in Southern South America—Emphasis in regional drought occurrences. *Adv. Geosci.* **2016**, *42*, 1–14, doi:10.5194/adgeo-42-1-2016.
40. Compagnucci, R.H.; Araneo, D.C. Identificación de áreas de homogeneidad estadística para los caudales de ríos andinos argentinos y su relación con la circulación atmosférica y la temperatura superficial del mar. *Meteorológica* **2005**, *30*, 41–53.
41. Caragunis, J.; Rivera, J.A.; Penalba, O. Variabilidad de baja frecuencia en los caudales de los ríos del centro-norte de Argentina y su contribución al desarrollo de sequías hidrológicas. In Proceedings of the XXVIII Reunión Científica de la Asociación Argentina de Geofísicos y Geodestas, La Plata, Buenos Aires, Argentina, 17–21 April 2017.
42. Penalba, O.C.; Rivera, J.A. Future changes in drought characteristics over Southern South America projected by a CMIP5 ensemble. *Am. J. Clim. Chang.* **2013**, *2*, 173–182, doi:10.4236/ajcc.2013.23017.
43. Rivera, J.A. Aspectos Climatológicos de las Sequías Meteorológicas en el Sur de Sudamérica. Análisis Regional y Proyecciones Futuras. Ph.D. Thesis, University of Buenos Aires, Buenos Aires, Argentina, 23 March 2014.
44. Rivera, J.A.; Araneo, D.C.; Penalba, O.C.; Villalba, R. Linking climate variations with the hydrological cycle over the semi-arid Central Andes of Argentina. Past, present and future, with emphasis on streamflow droughts. In *Geophysical Research Abstracts 19, EGU2017-995, Proceedings of the European Geosciences Union 2017 General Assembly, Vienna, Austria, 23–28 April 2017*; EGU: Vienna, Austria, 2017.
45. Historical El Niño/La Niña Episodes (1950–Present). Available online: http://www.cpc.ncep.noaa.gov/products/analysis_monitoring/ensostuff/ensoyears.shtml (accessed on 26 May 2017).
46. Smith, T.M.; Reynolds, R.W.; Peterson, T.C.; Lawrimore, J. Improvements to NOAA’s Historical Merged Land–Ocean Surface Temperature Analysis (1880–2006). *J. Clim.* **2008**, *21*, 2283–2296, doi:10.1175/2007JCLI2100.1.
47. Kalnay, E.; Kanamitsu, M.; Kistler, R.; Collins, W.; Deaven, D.; Gandin, L.; Iredell, M.; Saha, S.; White, G.; Woollen, J.; et al. The NCEP/NCAR 40-year reanalysis project. *Bull. Am. Meteorol. Soc.* **1996**, *77*, 437–470, doi:10.1175/1520-0477(1996)077<0437:TNYRP>2.0.CO;2.
48. Harpold, A.A.; Dettinger, M.; Rajagopal, S. Defining snow drought and why it matters. *Eos* **2017**, *98*, doi:10.1029/2017EO068775.
49. Snow Drought. Available online: <http://europeandroughtcentre.com/2017/04/20/snow-drought/> (accessed on 26 May 2017).
50. Masiokas, M.H.; Villalba, R.; Christie, D.A.; Betman, E.; Luckman, B.H.; Le Quesne, C.; Prieto, M.R.; Mauget, S. Snowpack variations since AD 1150 in the Andes of Chile and Argentina (30°–37° S) inferred from rainfall, tree-ring and documentary records. *J. Geophys. Res.* **2012**, *117*, D05112, doi:10.1029/2011JD016748.
51. Bianchi, L.; Rivera, J.; Rojas, F.; Britos Navarro, M.; Villalba, R. A regional water balance indicator inferred from satellite images of an Andean endorheic basin in central-western Argentina. *Hydrol. Sci. J.* **2017**, *62*, 533–545, doi:10.1080/02626667.2016.1247210.
52. Hong, X.; Guo, S.; Zhou, Y.; Xiong, L. Uncertainties in assessing hydrological drought using streamflow drought index for the upper Yangtze River basin. *Stoch. Environ. Res. Risk Assess.* **2015**, *29*, 1235–1247, doi:10.1007/s00477-014-0949-5.
53. Lorenzo-Lacruz, J.; Morán-Tejeda, E.; Vicente-Serrano, S.M.; López-Moreno, J.L. Streamflow droughts in the Iberian Peninsula between 1945 and 2005: Spatial and temporal patterns. *Hydrol. Earth Syst. Sci.* **2013**, *17*, 119–134, doi:10.5194/hess-17-119-2013.
54. Carril, A.F.; Doyle, M.E.; Barros, V.R.; Núñez, M.N. Impacts of climate change on the oases of the Argentinean cordillera. *Clim. Res.* **1997**, *9*, 121–129.
55. Lauro, C.; Vich, A.; Moreiras, S.M. Variabilidad del régimen fluvial en cuencas de la región de Cuyo. *Geoacta* **2016**, *40*, 28–51.
56. Mernild, S.H.; Liston, G.E.; Hiemstra, C.A.; Malmros, J.K.; Yde, G.C.; McPhee, J. The Andes Cordillera. Part I: Snow distribution, properties, and trends (1979–2014). *Int. J. Climatol.* **2017**, *37*, 1680–1698, doi:10.1002/joc.4804.

57. Masiokas, M.H.; Villalba, R.; Luckman, B.H.; Mauget, S. Intra- to multidecadal variations of snowpack and streamflow records in the Andes of Chile and Argentina between 30° and 37° S. *J. Hydrometeorol.* **2010**, *11*, 822–831, doi:10.1175/2010JHM1191.1.
58. Barnett, T.P.; Adam, J.C.; Lettenmaier, D.P. Potential impacts of a warming climate on water availability in snow-dominated regions. *Nature* **2005**, *438*, 303–309, doi:10.1038/nature0414.
59. Vicuña, S.; Garreaud, R.D.; McPhee, J. Climate change impacts on the hydrology of a snowmelt driven basin in semiarid Chile. *Clim. Chang.* **2011**, *105*, 469–488, doi:10.1007/s10584-010-9888-4.
60. Vicuña, S.; McPhee, J.; Garreaud, R.D. Agriculture Vulnerability to Climate Change in a Snowmelt-Driven Basin in Semiarid Chile. *J. Water Resour. Plan. Manag.* **2012**, *138*, 431–441, doi:10.1061/(ASCE)WR.1943-5452.0000202.
61. Rivera, J.A.; Araneo, D.C.; Penalba, O.C. Streamflow droughts over the central Andes of Argentina: Current crisis (2010–2014) in historical perspective. In Proceedings of the 11th International Conference on Southern Hemisphere, Santiago de Chile, Chile, 5–9 October 2015.



© 2017 by the authors. Licensee MDPI, Basel, Switzerland. This article is an open access article distributed under the terms and conditions of the Creative Commons Attribution (CC BY) license (<http://creativecommons.org/licenses/by/4.0/>).